European Journal of Pharmacology 649 (2010) 84–91

Contents lists available at ScienceDirect

European Journal of Pharmacology

journal homepage: www.elsevier.com/locate/ejphar

Molecular and Cellular Pharmacology

The flavonoid quercetin induces cell cycle arrest and mitochondria-mediated apoptosis in human cervical cancer (HeLa) cells through p53 induction and NF-κB inhibition

R. Vidya Priyadarsini [a], R. Senthil Murugan [a], S. Maitreyi [b], K. Ramalingam [b], D. Karunagaran [b], S. Nagini [a,*]

[a] Department of Biochemistry and Biotechnology, Faculty of Science, Annamalai University, Annamalainagar-608 002, Tamil Nadu, India
[b] Department of Biotechnology, Indian Institute of Technology, Chennai-600 036, Tamil Nadu, India

ARTICLE INFO

Article history:
Received 11 May 2010
Received in revised form 24 August 2010
Accepted 9 September 2010
Available online 19 September 2010

Keywords:
Quercetin
Cell cycle
Apoptosis
p53
NF-κB

ABSTRACT

With increasing use of plant-derived cancer chemotherapeutic agents, exploring the antiproliferative effects of phytochemicals has gained increasing momentum for anticancer drug design. The dietary phytochemical quercetin, modulates several signal transduction pathways associated with cell proliferation and apoptosis. The present study was undertaken to examine the effect of quercetin on cell viability, and to determine the molecular mechanism of quercetin-induced cell death by investigating the expression of Bcl-2 family proteins (Bcl-2, Bcl-xL, Mcl1, Bax, Bad, p-Bad), cytochrome C, Apaf-1, caspases, and survivin as well as the cell cycle regulatory proteins (p53, p21, cyclin D1), and NF-κB family members (p50, p65, IκB, p-IκB-α, IKKβ and ubiquitin ligase) in human cervical cancer (HeLa) cells. The results demonstrate that quercetin suppressed the viability of HeLa cells in a dose-dependent manner by inducing G2/M phase cell cycle arrest and mitochondrial apoptosis through a p53-dependent mechanism. This involved characteristic changes in nuclear morphology, phosphatidylserine externalization, mitochondrial membrane depolarization, modulation of cell cycle regulatory proteins and NF-κB family members, upregulation of proapoptotic Bcl-2 family proteins, cytochrome C, Apaf-1 and caspases, and downregulation of antiapoptotic Bcl-2 proteins and survivin. Quercetin that exerts opposing effects on different signaling networks to inhibit cancer progression is a classic candidate for anticancer drug design.

1. Introduction

Resistance to apoptosis, a frequent challenge in human malignancies contributes to cancer development by promoting cell survival and resistance to antineoplastic drugs (Akgul, 2009). New anticancer therapeutic regimens are therefore focused on the selective induction of tumour cell death through activation of the apoptotic pathway (Plati et al., 2008). Apoptosis, a form of programmed cell death characterized by stereotypical morphological changes including membrane blebbing, cell shrinkage, nuclear fragmentation, and chromatin condensation is executed by caspases and regulated by the Bcl-2 family members (Burz et al., 2009; Schultz and Harrington, 2003). The hierarchical activation of caspases results in cleavage of proteins vital for cell survival leading to morphological and biochemical changes characteristic of apoptotic cell death (Logue and Martin, 2008). Several molecules including members of the Bcl-2 family, survivin, as well as nuclear factor kappa B (NF-κB) function as key regulators of apoptosis (Yip and Reed, 2008; Mita et al., 2008; Sethi et al., 2008).

The delicate balance between the relative levels of proapoptotic members of the Bcl-2 family that activate the caspase cascade by creating pores in the mitochondrial membrane with release of cytochrome C, and antiapoptotic proteins that prevent cytochrome C release is a critical determinant of cell fate (Akgul, 2009; Chipuk and Green, 2008; Brunelle and Letai, 2009). Survivin, a predominant member of the inhibitor of apoptosis protein (IAP) family, blocks apoptosis by interacting with and inactivating the proapoptogenic mitochondrial protein SMAC (second mitochondria-derived activator of caspase) and by inhibiting caspases (Ceballos-Cancino et al., 2007). NF-κB, a prosurvival transcription factor inhibits apoptosis by influencing the expression of antiapoptotic Bcl-2 members and IAPs (Pahl, 1999). In resting cells, NF-κB exists in the cytoplasm as a heterodimer composed of p50 and p65 subunits complexed to IκB. Phosphorylation of IκB by IKKβ followed by ubiquitination and proteasomal degradation activates NF-κB with consequent nuclear translocation and activation of antiapoptotic genes (Shen and Tergaonkar, 2009).

Dietary phytochemicals that selectively perturb cellular pathways and restore apoptosis in tumour cells have attracted research interest

* Corresponding author. Tel.: +91 4144 239842; fax: +91 4144 238145/238080.
E-mail addresses: s_nagini@yahoo.com, snlabau@gmail.com (S. Nagini).

0014-2999/$ – see front matter © 2010 Elsevier B.V. All rights reserved.
doi:10.1016/j.ejphar.2010.09.020

in recent years for novel apoptosis-based therapies (Khan et al., 2008). Various dietary agents including curcumin, resveratrol, tea polyphenols, and flavonoids have been reported to induce apoptosis in a wide range of tumours (Watson et al., 2010; Chakraborty et al., 2008; Letchoumy et al., 2007; Kim et al., 2009). Quercetin (3,3′,4′,5,7-pentahydroxyflavone), a flavone-3ol-class of flavonoid, ubiquitously present in fruits and vegetables, has been reported to modulate signal transduction pathways associated with cell proliferation and apoptosis (Murakami et al., 2008). Quercetin-induced cell cycle arrest at G1/S or G2/M phase has been documented in various cancer cell types (Ranelletti et al., 1992; Yoshida et al., 1992; Avila et al., 1994; Yang et al., 2006). Furthermore, quercetin-induced apoptotic cell death has been evaluated in several human cancer cell lines including glioma, liver, lung, prostate, and colon cancer cells by focusing on the Bcl-2 family members and/or caspases (Kim et al., 2008; Tanigawa et al., 2008; Lee et al., 2008; Kim et al., 2005). These reports although invaluable, are invariably incomplete as the precise molecular mechanisms underlying quercetin-induced antiproliferation and apoptosis still remain to be delineated. The present study was undertaken to determine the molecular mechanism of quercetin-induced cell death by investigating Bcl-2 family proteins, cytochrome C, Apaf-1, caspases (-3 and -9) and survivin as well as the cell cycle regulatory proteins p53, p21, cyclin D1, and NF-κB family members in human cervical cancer (HeLa) cells.

2. Materials and methods

2.1. Chemicals

Acridine orange, 4,6-diamidino-2-phenylindol (DAPI), 2′,7′-dichlorofluorescein diacetate (DCFH-DA), diethyl pyrocarbonate (DEPC), reduced glutathione (GSH), ethidium bromide, JC-1 iodide, MTT (3-(4,5-dimethylthiazol-2-yl)-2-5-diphenyltetrazoliumbromide), quercetin dehydrate and RNase A were purchased from Sigma Chemical Company, St. Louis, MO, USA. Stock solution of quercetin (100 mM) prepared by dissolving in 0.5% DMSO was diluted with Dulbecco's modified Eagles medium (DMEM) prior to use to obtain the desired concentration. The final concentration of DMSO used for treatment was 0.1% (v/v).

2.2. Cell culture and maintenance

HeLa cells were procured from the National Centre for Cell Science, Pune, India. The cells were grown in DMEM (GIBCO BRL, Grand Island, NY, USA) containing 10% FBS (Sigma, USA) and antibiotics (100 U/ml of penicillin and 100 μg/ml of streptomycin). Cells were maintained as monolayer cultures in a humidified atmosphere of 5% CO_2 at 37 °C.

2.3. Determination of cell viability

Cell viability was assessed by the MTT assay based on the reduction of MTT by mitochondrial dehydrogenases of viable cells to a purple formazon product (Mosmann, 1983). Briefly, cells were plated at a density of 1×10^5 cells/ml into 96-well plates. After overnight growth, cells were treated with 20, 40, 60, 80 and 100 μM concentrations of quercetin for 24 h. Subsequently, the cells were washed with 200 μl of PBS, and incubated with 100 μl of 500 μg/ml MTT in PBS at 37°C for 3 h. The MTT-formazon product dissolved in 200 μl of DMSO was estimated by measuring the absorbance at 570 nm in an ELISA plate reader. The percent of cell survival was determined by comparing the average absorbance of the treated cells with the corresponding absorbance of untreated cells. All doses were tested in triplicates and the experiment was repeated at least three times.

2.4. Cell cycle analysis

HeLa cells were seeded in 6-well plates at a seeding density of 5×10^4 cells/ml. Cells were pre-incubated for overnight and then treated with or without quercetin (80 μM) for 24 h. Cells were harvested by trypsinization, collected, and fixed in ice-cold 70% ethanol for at least 1 h at 4°C. The cells were centrifuged to remove ethanol and washed again with cold PBS. The pellets were resuspended in 1 ml PI solution (0.1% Triton X-100, 0.1 mM EDTA, 50 μg/ml PI in PBS) containing 50 μg/ml RNase, and then incubated in the dark at 37°C for 30 min and protected from light. Stained cells were incubated at room temperature for 30 min. The DNA content was analyzed using a Beckman-Coulter Quanta™ SC MPL flow cytometry. Data presented are representative of those obtained in at least three independent experiments done in triplicates.

2.5. Acridine orange/ethidium bromide staining

Characteristic apoptotic morphological changes were assessed by fluorescent microscopy using acridine orange/ethidium bromide (AO/EB) staining. Briefly, cells were seeded in 12-well plate at seeding densities of 1×10^5 cells and then treated with quercetin (80 μM) for 24 h. After washing once with phosphate buffered saline (PBS), the cells were washed with 100 μl of 1:1 mixture of acridine orange/ethidium bromide (4 μg/ml) solutions. The cells were immediately washed with DMEM, viewed, and photographed using Nikon inverted fluorescent microscope (TE-Eclipse 300). Viable cells stained only by AO were bright green with intact structure; apoptotic cells stained by AO_{LOW} and EB were red-orange with condensation of chromatin as dense orange areas and reduced cells. Data presented are representative of those obtained in at least three independent experiments done in triplicates.

2.6. Nuclear morphology

The changes in the nuclear morphology of cells following exposure to quercetin (80 μM) were examined using the DNA-specific fluorochrome DAPI. Cells were plated at a density of 1×10^5 cells/well in a 12-well plate. After 24 h of exposure to quercetin, the cells were fixed in ice-cold methanol (−20°C) for 15 min and stained with DAPI (1 μg/ml) for 30 min in dark. Nuclear morphology of apoptotic cells with condensed/fragmented nuclei was examined under a fluorescent microscope (Nikon TE-Eclipse 300) and at least 1×10^3 cells were counted for assessing apoptotic cell death. Data presented are representative of those obtained in at least three independent experiments done in triplicates.

2.7. Annexin V-FITC-PI assay

The number of apoptotic cell death induced by quercetin was measured by flow cytometry using annexin V-FITC-PI kit (Sigma). The annexin V-PI assay evaluates phospholipid turnover from the inner to the outer lipid layer of the plasma membrane, an event typically associated with apoptosis. Briefly, control and quercetin (80 μM) treated cells were harvested and washed with cold PBS. The cell pellet was resuspended in 1× binding buffer at a concentration of 1×10^6 cells/ml. To 100 μl of cell suspension 5 μl of Annexin V-FITC and 5 μl of PI were added and vortexed gently. The stained samples were incubated for 15 min at room temperature in the darkness. An additional 400 μl of 1× binding buffer was added to each tube. Samples were analyzed by Beckman-Coulter Quanta™ SC MPL flow cytometry within 1 h. A total of 100,000 events were acquired using green channel FL1 for Annexin V-FITC and the red channel FL3 for PI. The experiment was repeated at least three times in triplicates. Data presented are representative of those obtained in at least three independent experiments done in triplicates.

Table 1
Oligonucleotide primers and thermocycling conditions for RT-PCR.

Gene product	Primer sequences	Product size (bp)	Annealing temperature	No. of cycles
Apaf-1	Sense 5′-CACGTTCAAAGGTGGCTGAT-3′ Antisense 5′-TGGTCAACTGCAAGGACCAT-3′	170	60 °C, 30 s	30
Bad	Sense 5′-CCCAGAGTTTGAGCCGAGTG-3′ Antisense 5′-GCTGTGCTGCCCAGAGGTT-3′	317	57 °C, 1 min	30
Bax	Sense 5′-ACCAAG CTGAGCGA GTGTC-3′ Antisense 5′-ACAAAGATGGTCACGGTCTGCC-3′	293	60 °C, 1 min	28
Bcl-2	Sense 5′-ACCAAG CTGAGCGA GTGTC-3′ Antisense 5′-ACAAAGATGGTCACGGTCTGCC-3′	415	60 °C, 1 min	26
Bcl-xL	Sense 5′-GAGGCAGGCGACGAGTTT-3′ Antisense 5′-GACGGAGGATGTGGTGGA-3′	320	58 °C, 1 min	28
Caspase-3	Sense 5′-GACAACAACGAAACCTCCGT-3′ Antisense 5′-GACTTCGTATTTCAGGGCCA-3′	382	60 °C, 45 s	30
Caspase-9	Sense 5′-TGTGGTGGTCATCCTCTCTCA-3′ Antisense 5′-GTCACTGGGGGTAGGCAAACT-3′	282	66 °C, 1 min	30
Cyclin D1	Sense 5′-CGGAGGACAACAAACAGATC-3′ Antisense 5′-GGGTGTGCAAGCCAGGTCCA-3′	331	57 °C, 45 s	28
Cytochrome C	Sense 5′-GGAGGCAAGCATAAGACTGG-3′ Antisense 5′-GTCTGCCCTTTCTCCCTTCT-3′	267	56 °C, 1 min	30
p21	Sense 5′-CTCAGAGGAGGCGCCATG-3′ Antisense 5′-GGGCGGATTAGGGCTTCC-3′	517	60 °C, 1 min 20 s	26
p53	Sense 5′-GTTTCCGTCTGGGCTTCTTG-3′ Antisense 5′-CCTGGGCATCCTTGAGTTCC-3′	473	64 °C, 1 min	30
PCNA	Sense 5′-GCCCTCAAAGACCTCATCAA-3′ Antisense 5′-GCTCCCCACTCGCAGAAAAC-3′	472	60 °C, 30 s	28
β-Actin	Sense 5′-AACCGCGAGAAGATGACCCAGATCATGTTT-3′ Antisense 5′-AGCAGCCGTGGCCATCTCTTGCTCGAAGTC-3′	350	60 °C, 1 min	30

2.8. Analysis of mitochondrial transmembrane potential

The changes in the mitochondrial transmembrane potential ($\Delta\psi M$) were determined using JC-1, a fluorescent carbocyanine dye, which accumulates in the mitochondrial membrane as a monomer or dimer depending on the mitochondrial membrane potential (Smiley et al., 1991). Briefly, cells were plated at a seeding density of 2×10^5 cells/well in a 12-well plate. After 24 h of quercetin treatment, cells were incubated with 5 μM JC-1 for 30 min at room temperature in the dark. The presence of JC-1 monomers or dimers was examined under a fluorescent microscope using filter pairs of 530/590 nm (dimers) and 485/538 nm (monomers). Data presented are representative of those obtained in at least three independent experiments done in triplicates.

2.9. Determination of reactive oxygen species generation

To determine whether the mitochondrial membrane depolarization was associated with reactive oxygen species generation, the changes in intracellular reactive oxygen species generation were measured using fluorometric DCFH assay as described by Wang et al. (1999). Briefly, a stock solution of DCFH-DA (1 mM) was prepared in DMSO, aliquoted, and stored at −20°C. An amount of 10 μM DCFH-DA was freshly prepared by diluting the stock solution with medium for analysis. Cells were treated with or without IC_{50} concentration of quercetin for 24 h. Subsequently, cells were trypsinized, harvested and suspended in 0.5 ml DMEM containing 10 μM DCFH-DA for 15 min at 37°C in the dark. After 15 min, cells were placed in a Perkin-Elmer LS 5B fluorimeter (Perkin-Elmer, Germany) and the intensity of DCF fluorescence was recorded for 30 min using 485/530 nm excitation/emission filter. DCFH-DA is taken up by cells and deacetylated by cellular esterase to form a non-fluorescent product DCFH. DCFH is converted to a green fluorescent product DCF by intracellular reactive oxygen species produced by treated cells. The percentage increase of fluorescence intensity was calculated using the formula [(fluorescence at time 30 min − fluorescence at time 0 min)/fluorescence at time 0 min × 100]. Reactive oxygen species levels were expressed as percentage over control. The experiment was replicated three different times.

2.10. RNA isolation and cDNA synthesis

Following treatment, cells grown in 60 mm Petri dishes were washed with ice-cold PBS and 1 ml of trizol was added and flushed gently to disrupt the cells. The lysates were collected and mixed with 300 μl of chloroform by inversion. The tubes were then centrifuged at 10,000 rpm for 15 min at 4°C. The aqueous phases from the tubes were collected and the RNA was precipitated using 700 μl of isopropanol and centrifuged at 10,000 rpm for 10 min at 4 °C. The pellets were washed twice with 70% ethanol and air-dried for about 20–40 min. The pellets were resuspended in 100 μl of DEPC treated water. The purity of RNA was checked by $OD_{260/280}$ of RNA samples (>1.8). The quality of the RNA was analyzed by agarose gel electrophoresis.

Isolated total RNA (1 μg) was reverse-transcribed to cDNA in a reaction mixture containing 4 μl of 5× reaction buffer, 2 μl of dNTPs mixture (10 mM), 20 units of RNase inhibitor, 200 units of avian-myeloblastosis virus (AMV) reverse transcriptase and 0.5 μg of oligo (dT) primer (Promega, WI, USA) in a total volume of 20 μl. The

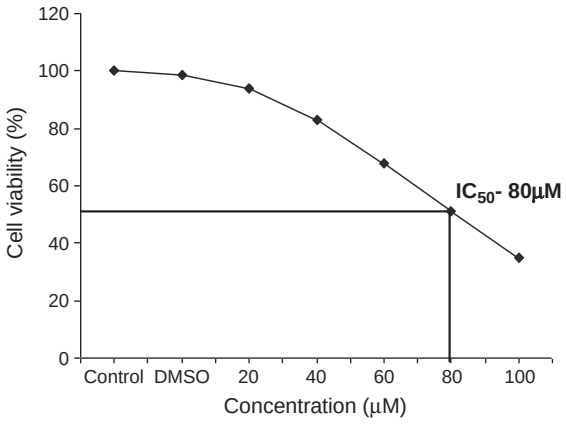

Fig. 1. Effect of quercetin on viability of HeLa cells. Data are represented as mean ± SD of three determinations each performed in triplicate.

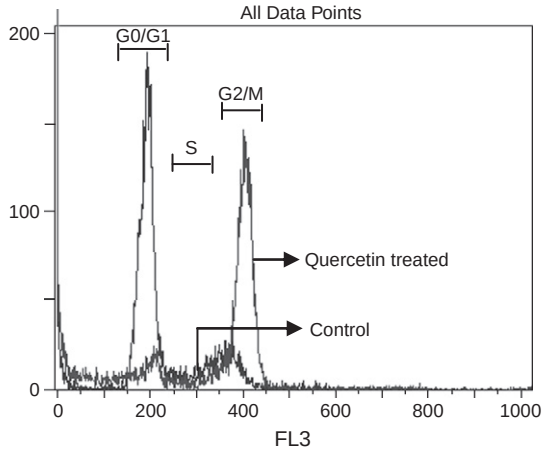

Fig. 2. Flow cytometric analysis of the effect of quercetin on cell cycle of HeLa cells. The data presented are representative of three independent experiments.

reaction mixture was incubated at 42°C for 60 min and the reaction was terminated by heating at 70°C for 10 min. The resultant cDNA was stored at −80°C until further use.

2.11. PCR amplification

All oligonucleotide primers were purchased from Sigma Genosys, India. Details about the primers are given in Table 1. The PCR amplification reaction mixture (in a final volume of 25 μl) contained 1 μl of cDNA, 0.5 μl of forward primer, 0.5 μl of reverse primer and 10 μl of Hot Master Mix (2.5×) (Eppendorf, Hamburg, Germany). The PCR was carried out in a thermal cycler (Eppendorf). Negative controls without cDNA were also performed. Amplification products were analyzed by electrophoresis in a 2% agarose gel containing ethidium bromide with 100 bp DNA ladder. The PCR products were visualized as bands with a UV-transilluminator and photographs were taken using gel documentation system (GelDocMega™, United Kingdom). The PCR products were quantitated with Total Lab 1.11 software following densitometric analysis.

2.12. Western blot analysis

Following treatment, cells were washed three times with PBS and lysed in a RIPA lysis buffer [50 mM Tris–HCl (pH 7.4), 1% Nonidet P-40, 40 mM NaF, 10 mM NaCl, 10 mM Na_3VO_4, 1 mM phenylmethanesulfonyl fluoride (PMSF), and 10 mM dithiothreitol (DTT)]. The cell lysates were centrifuged at 14,000 rpm for 15 min.

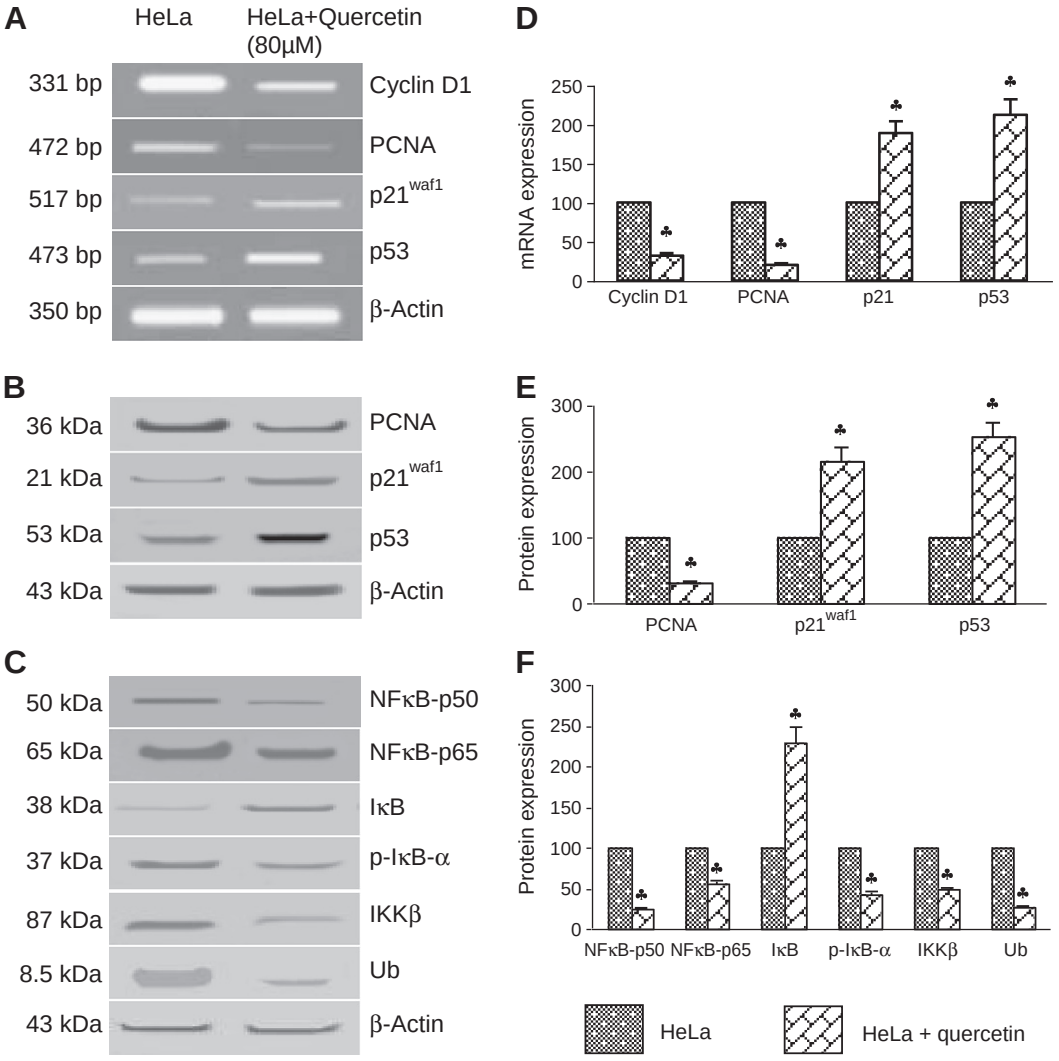

Fig. 3. Effect of quercetin on markers of cell proliferation and survival and expression of NF-κB family members in HeLa cells. A. Representative RT-PCR analyses. β-actin was used as an internal control. B, C. Representative immunoblots. Protein samples (50 μg/lane) resolved on SDS–PAGE were probed with antibodies. β-actin was used as loading control. D, E, F. Densitometric analysis. ♣ Significantly different from HeLa ($p<0.01$) by Student's *t*-test.

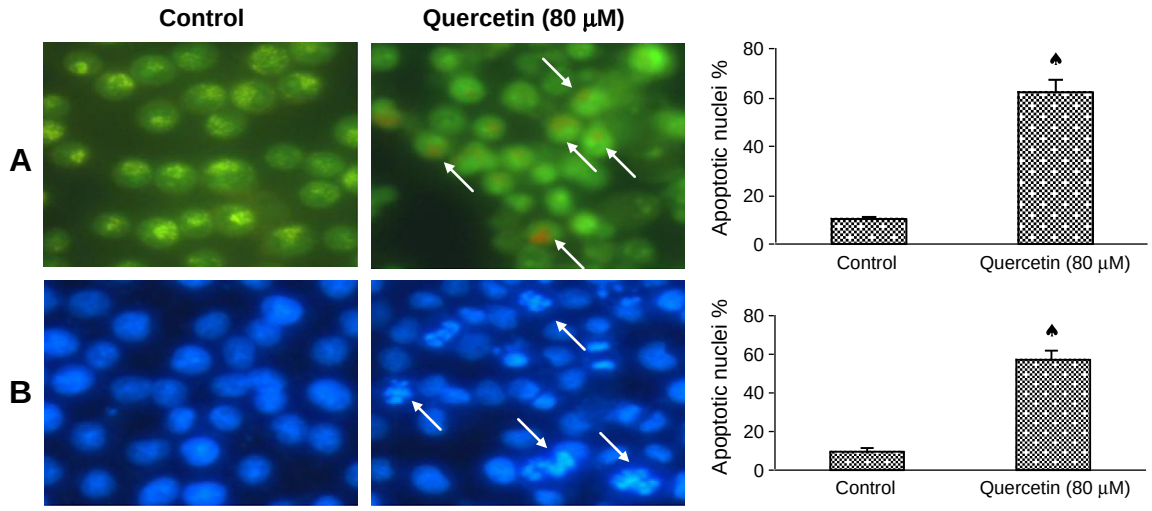

Fig. 4. Morphological changes and the number of apoptotic nuclei formed after treatment with quercetin for 24 h. A—AO/EB staining, B—DAPI staining. Error bar represents SD between counts of three independent experiments. Apoptotic cells are shown as white arrowheads. ♠ Significantly different from control ($p<0.001$) by Student's *t*-test.

For the preparation of mitochondrial fraction, cells treated with quercetin (80 μM) were washed with PBS and homogenized using the homogenizing buffer (10 mM HEPES (pH 7.9), 10 mM KCl, 0.1 mM EDTA, 0.1 mM EGTA, 1 mM DTT, 0.5 mM PMSF). The homogenate was centrifuged at 1000×*g* for 5 min to remove the nuclear and unbroken cells. The supernatant was centrifuged at 23,100×*g* for 30 min at 4°C, the resulting supernatant was collected and the pellet containing mitochondria was resuspended in lysis buffer (150 mM NaCl, 0.5% triton X-100, 50 mM Tris, 20 mM EGTA, 1 mM DTT, 1 mM sodium orthovanadate, and protease inhibitor cocktail). Total protein was determined by the method of Bradford (1976). A total of 55 μg of this suspension was used for western blot analysis.

Proteins separated by SDS–PAGE were electrophoretically transferred to polyvinylidene difluoride membranes. The membranes were incubated in 1× PBS containing 5% non-fat dry milk for 2 h to block non-specific binding sites. The blots were incubated with 1:300 dilutions of primary antibodies (Santa Cruz Biotechnology, CA, USA) for 30–45 min at room temperature. After washing, the blots were incubated with 1:1000 dilutions of horseradish peroxidase-conjugated secondary antibodies (Santa Cruz Biotechnology, CA, USA) for 45 min at room temperature. After extensive washes with high and low salt buffers, the immunoreactive proteins were visualized using enhanced chemiluminescence (ECL) detection reagents (Sigma). Densitometry was performed on IISP flat bed scanner and quantitated with Total Lab 1.11 software.

2.13. Statistical analysis

Cytotoxicity data are presented as mean percentages of control ± SD. The data for apoptosis, RT-PCR and western blot were analyzed by Student's *t*-test. The results were considered statistically significant if the *p* value was <0.05.

3. Results

3.1. Effect of quercetin on cell viability

Incubation of cells for 24 h with quercetin (20–100 μM) significantly decreased cell survival in a dose-dependent manner (Fig. 1). Reduction in cell viability by ~50% in comparison with the control was achieved at a dose of 80 μM. In contrast to quercetin treated cells, cells treated with DMSO showed little or no cytotoxicity.

3.2. Effect of quercetin on cell cycle and cell proliferation

Analysis of cell cycle indicated that treatment of cells for 24 h with quercetin (80 μM) increased the percentage of cells in G2/M phase and decreased the percentage of cells in G1 and S phases (Fig. 2). Western blot and RT-PCR analysis of the expression of p53, p21, cyclin D1, PCNA, and NF-κB family members (p50, p65, IκB, p-IκB-α, IKKβ, Ub) revealed a significant increase in the expression

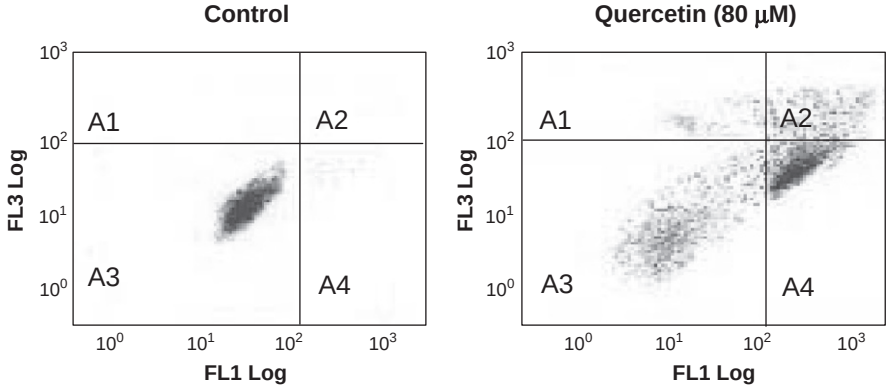

Fig. 5. Scatter plots of Annexin V-FITC/PI stained control and cells treated with quercetin under four situations in a quadrant analysis. A1—necrotic or dead cells, A2—late apoptotic or dead cells, A3—living cells, A4—early apoptotic cells. The data presented are representative of three independent experiments. * Significantly different from group 8 ($p<0.001$) ANOVA followed by LSD.

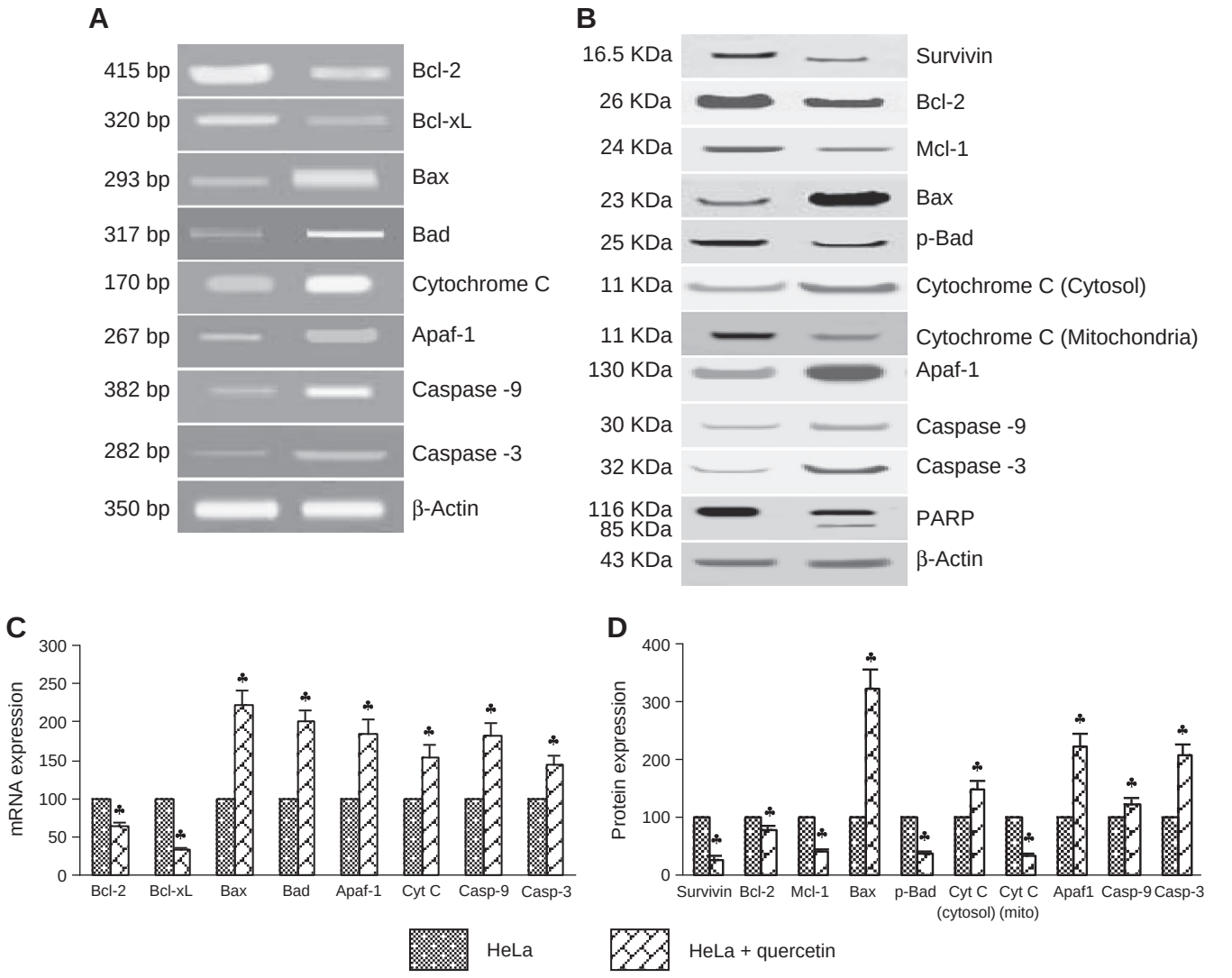

Fig. 6. Effect of quercetin on markers of intrinsic apoptosis in HeLa cells. A. Representative RT-PCR analyses. β-actin was used as an internal control. B. Representative immunoblots. Protein samples (50 μg/lane) resolved on SDS–PAGE were probed with antibodies. β-actin was used as loading control. C, D. Densitometric analysis. ♣ Significantly different from HeLa ($p<0.01$) by Student's *t*-test.

of p53, p21, and IκB, with a decrease in the expression of cyclin D1, PCNA, NF-κB (p50 and p65), p-IκB-α, IKKβ and Ub in HeLa cells treated with quercetin compared to untreated control (Fig. 3).

3.3. Effect of quercetin on cell and nuclear morphology and phosphatidylserine

Treatment of cells with quercetin (80 μM) for 24 h resulted in cell shrinkage, chromosomal condensation, nuclear and plasma membrane convulsion and nuclear fragmentation indicating that the cytotoxic action of quercetin was due to its ability to induce apoptosis (Fig. 4). Analysis of control and quercetin (80 μM) treated cells by annexin V-PI assay indicated that the proportion of annexin V stained cells increased from 0.13% (control) to 36.9% in quercetin treated cells (Fig. 5).

3.4. Effect of quercetin on markers of intrinsic apoptosis

Analysis of survivin, Bcl-2 family members (Bcl-2, Bcl-xL, Mcl-1, Bax, Bad, p-Bad), cytochrome C (mitochondrial and cytosolic), Apaf-1, caspases (-9 and -3), and PARP cleavage by RT-PCR and western blot analyses revealed a significant increase in the expression of Bax, Bad, cytosolic cytochrome C, Apaf-1, caspase -9 and -3, and PARP cleavage with decrease in the expression of survivin, Bcl-2, Bcl-xL, Mcl-1, p-Bad and mitochondrial cytochrome C in cells treated with quercetin compared to untreated control (Fig. 6).

3.5. Effect of quercetin on mitochondrial transmembrane (ΔΨM) potential

Treatment of cells with quercetin (80 μM) for 24 h resulted in the depolarization of the mitochondrial membrane potential as revealed by a change in fluorescence from red to green, compared to control (Fig. 7A).

3.6. Role of reactive oxygen species in quercetin-induced cell death

Treatment of cells for 24 h with 80 μM quercetin did not induce any significant changes in reactive oxygen species generation compared to untreated control (Fig. 7B). Analysis of the effect of the antioxidant GSH on cell viability revealed that quercetin-induced loss of cell viability was not affected by the addition of GSH, indicating that

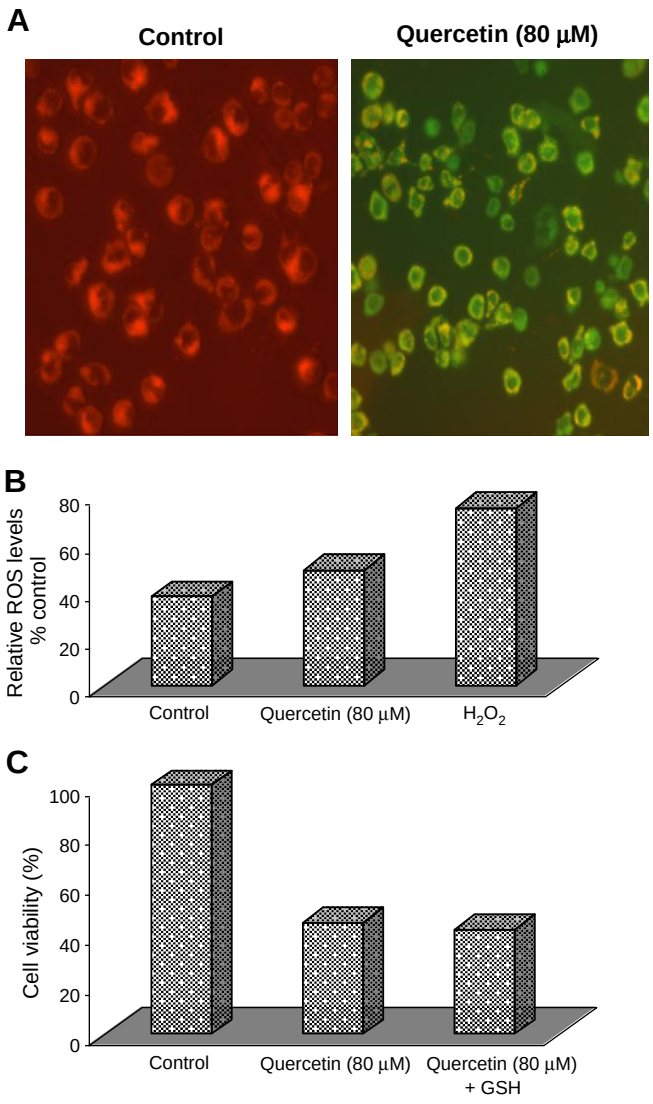

Fig. 7. A. Effect of quercetin on mitochondrial transmembrane potential. Fluorescent microscopy images of control cells (left panel) and cells treated with IC_{50} concentration of quercetin for 2 h at 37 °C (right panel). Reddish-orange fluorescence of JC-1 dimers is seen in cell areas with high mitochondrial membrane potential, while green fluorescence of JC-monomers is prevalent in the cell areas with low mitochondrial membrane potential. The JC-1 stained cells were visualized under an inverted fluorescence microscope. B. Effect of quercetin (80 μM) on reactive oxygen species generation as determined by DCFH-DA assay. The values represent mean ± SD of three independent experiments ($p<0.05$). C. Effect of antioxidants on quercetin-induced loss of cell viability. Cell viability was determined as described in the Materials and methods section. The values represent mean ± SD of three independent experiments ($p<0.05$).

quercetin-induced cell death is not associated with reactive oxygen species generation (Fig. 7C).

4. Discussion

With increasing use of plant-derived cancer chemotherapeutic agents such as vinblastine, adriamycin and paclitaxel, exploring the antiproliferative effects of phytochemicals has gained increasing momentum for anticancer drug design (Da Rocha et al., 2001). In the present study, the plant flavonoid quercetin exerted potent antiproliferative effects on HeLa cells with an IC_{50} value of 80 μM. Several researchers have documented the cytotoxic and antiproliferative effects of quercetin in various human cancer cell lines (Chien et al., 2009; Kang et al., 2010; Zhang and Zhang, 2009; Shan et al., 2009). Zhang et al. (2009) investigated the cytotoxic effect of three structurally related flavonoids—quercetin, kaempferol and myricetin in KYSE-150 cells and found quercetin to be the most potent cytotoxic flavonoid with an IC_{50} value of 48 μM. Quercetin was shown to exert cytotoxic effects at concentrations ranging from 30 to 100 μM in diverse cancer cell lines (Ranelletti et al., 1992; Yoshida et al., 1992; Avila et al., 1994; Yang et al., 2006; Kim et al., 2008; Tanigawa et al., 2008; Lee et al., 2008; Kim et al., 2005). Our data are consistent with the IC_{50} value of 76.1 μM reported by Tanigawa et al. (2008) in HepG2 cells. The differences in IC_{50} values of quercetin in individual cell lines may be attributed to the differences in the duration of exposure and the differential sensitivities of cell lines to the cytotoxic effects of quercetin.

Analysis of the cell cycle revealed perturbation at G2/M phase, the crucial phase of mitotic cell cycle controlled by cyclins and cyclin-dependent kinases. While cyclins and CDKs regulate the progression of cell cycle from G2/M to S phase, the tumour suppressor p53 and its downstream target $p21^{waf1}$, a potent cyclin–CDK inhibitor induces cell cycle arrest (Hall and Peters, 1996; Fuster et al., 2007). The results of the present study provide evidence for a p53–p21 mediated cell cycle arrest at G2/M phase by quercetin. These findings are similar to those documented in HepG2 and NCI-H209 cells by other workers (Yang et al., 2006; Tanigawa et al., 2008).

In addition to G2/M arrest, cells exposed to quercetin exhibited morphological changes characteristic of apoptosis such as phosphatidylserine externalization, decline in the mitochondrial membrane potential, nuclear fragmentation and chromatin condensation. The decrease in the Bcl-2/Bax ratio induced by quercetin was independent of reactive oxygen species production. In addition, dephosphorylation of Bad may contribute to mitochondrial apoptosis by facilitating dissociation of Bax from Bcl-xL, and subsequent Bax oligomerization into the mitochondrial membrane (Lalier et al., 2007). The upregulation of cytochrome C, Apaf-1, and caspases together with PARP cleavage, a hallmark of apoptosis, supports the formation of the apoptosome complex and activation of the caspase cascade. Recent studies have indicated that p53 can inhibit antiapoptotic Bcl-xL promoting cytochrome C release in addition to stimulating Bax oligomerization (Mihara et al., 2003; Chipuk et al., 2004).

In contrast to p53, activation of the pro-survival transcription factor NF-κB promotes cancer cell survival by triggering apoptosis evasion (Naugler and Karin, 2008). Constitutive activation of NF-κB negatively regulates the proapoptotic functions of p53 by inducing the expression of an array of antiapoptotic genes including Bcl-2, Bcl-xL, and survivin (Sethi et al., 2008; Naugler and Karin, 2008). Enhanced IκB expression together with downregulated expression of NF-κB, IKKβ, p-IκB and Ub, seen in the present study provides a mechanistic basis for the inactivation of NF-κB by quercetin. Consistent with this report, several dietary agents such as curcumin, and resveratrol have been demonstrated to abrogate NF-κB activation in tumour cells via IκB phosphorylation and degradation (Divya and Pillai, 2006; Kundu et al., 2006).

In conclusion, the results of the present study reveal that quercetin inhibits HeLa cell proliferation through cell cycle arrest at G2/M phase and apoptosis induction through the disruption of $\Delta\Psi M$, and activation of the intrinsic apoptotic pathway. Our results also indicate that quercetin simultaneously targets two opposing signaling networks—p53 and NF-κB to inhibit cancer progression in HeLa cells. Recent studies have demonstrated that agents that simultaneously target p53 and NF-kappaB pathways are efficient as cancer therapeutics (Dey et al., 2008). The ability of quercetin to inhibit cancer progression via p53 induction and NF-κB inhibition suggests that quercetin could be a classic candidate for anticancer drug design.

Conflict of interest

None

Acknowledgement

Financial support from the Indian Council of Medical Research, New Delhi, India in the form of a Senior Research Fellowship to Ms. R. Vidya Priyadarsini is gratefully acknowledged.

References

Akgul, C., 2009. Mcl-1 is a potential therapeutic target in multiple types of cancer. Cell. Mol. Life Sci. 66, 1326–1336.
Avila, M.A., Velasco, J.A., Cansado, J., Notario, V., 1994. Quercetin mediates the down-regulation of mutant p53 in the human breast cancer cell line MDA-MB468. Cancer Res. 54, 2424–2428.
Bradford, M.M., 1976. A rapid and sensitive method for the quantitation of microgram quantities of protein utilizing the principle of protein-dye binding. Anal. Biochem. 72, 248–254.
Brunelle, J.K., Letai, A., 2009. Control of mitochondrial apoptosis by the Bcl-2 family. J. Cell Sci. 122, 437–441.
Burz, C., Berindan-Neagoe, I., Balacescu, O., Irimie, A., 2009. Apoptosis in cancer: key molecular signaling pathways and therapy targets. Acta Oncol. 488, 11–21.
Ceballos-Cancino, G., Espinosa, M., Maldonado, V., Melendez-Zajgla, J., 2007. Regulation of mitochondrial Smac/DIABLO-selective release by survivin. Oncogene 26, 7569–7575.
Chakraborty, P.K., Mustafi, S.B., Ganguly, S., Chatterjee, M., Raha, S., 2008. Resveratrol induces apoptosis in K562 (chronic myelogenous leukemia) cells by targeting a key survival protein, heat shock protein 70. Cancer Sci. 99, 1109–1116.
Chien, S.Y., Wu, Y.C., Chung, J.G., Yang, J.S., Lu, H.F., Tsou, M.F., Wood, W.G., Kuo, S.J., Chen, D.R., 2009. Quercetin-induced apoptosis acts through mitochondrial- and caspase-3-dependent pathways in human breast cancer MDA-MB-231 cells. Hum. Exp. Toxicol. 28, 493–503.
Chipuk, J.E., Green, D.R., 2008. How do BCL-2 proteins induce mitochondrial outer membrane permeabilization? Trends Cell Biol. 18, 157–164.
Chipuk, J.E., Kuwana, T., Bouchier-Hayes, L., Droin, N.M., Newmeyer, D.D., Schuler, M., Green, D.R., 2004. Direct activation of Bax by p53 mediates mitochondrial membrane permeabilization and apoptosis. Science 303, 1010–1014.
Da Rocha, A.B., Lopes, R.M., Schwartsmann, G., 2001. Natural products in anticancer therapy. Curr. Opin. Pharmacol. 1, 364–369.
Dey, A., Tergaonkar, V., Lane, D.P., 2008. Double-edged swords as cancer therapeutics: simultaneously targeting p53 and NF-kappaB pathways. Nat. Rev. Drug Discov. 7, 1031–1040.
Divya, C.S., Pillai, M.R., 2006. Antitumor action of curcumin in human papilloma virus associated cells involve downregulation of viral oncogenes, prevention of NF-KB and AP-1 translocation and modulation of apoptosis. Mol. Carcinog. 45, 320–332.
Fuster, J.J., Sanz-González, S.M., Moll, U.M., Andrés, V., 2007. Classic and novel roles of p53: prospects for anticancer therapy. Trends Mol. Med. 13, 192–199.
Hall, M., Peters, G., 1996. Genetic alterations of cyclins, cyclin-dependent kinases, and Cdk inhibitors in human cancer. Adv. Cancer Res. 68, 67–108.
Kang, J.W., Kim, J.H., Song, K., Kim, S.H., Yoon, J.H., Kim, K.S., 2010. Kaempferol and quercetin, components of Ginkgo biloba extract (EGb 761), induce caspase-3-dependent apoptosis in oral cavity cancer cells. Phytother. Res. 1, S77–82.
Khan, N., Adhami, V.M., Mukhtar, H., 2008. Apoptosis by dietary agents for prevention and treatment of cancer. Biochem. Pharmacol. 76, 1333–1339.
Kim, E.J., Choi, C.H., Park, J.Y., Kang, S.K., Kim, Y.K., 2008. Underlying mechanism of quercetin-induced cell death in human glioma cells. Neurochem. Res. 33, 971–979.
Kim, S.H., Kim, S.H., Lee, S.C., Song, Y.S., 2009. Involvement of both extrinsic and intrinsic apoptotic pathways in apoptosis induced by genistein in human cervical cancer cells. Ann. NY Acad. Sci. 1171, 196–201.
Kim, W.K., Bang, M.H., Kim, E.S., Kang, N.E., Jung, K.C., Cho, H.J., Park, J.H., 2005. Quercetin decreases the expression of ErbB2 and ErbB3 proteins in HT-29 human colon cancer cells. J. Nutr. Biochem. 16, 155–162.
Kundu, J.K., Shin, Y.K., Surh, Y.J., 2006. Resveratrol modulates phorbol ester induced proinflammatory signal transduction pathways in mouse skin in vivo: NF-KappaB and AP-1 as prime targets. Biochem. Pharmacol. 72, 1506–1515.
Lalier, L., Cartron, P.F., Juin, P., Nedelkina, S., Manon, S., Bechinger, B., Vallette, F.M., 2007. Bax activation and mitochondrial insertion during apoptosis. Apoptosis 12, 887–896.
Lee, D.H., Szczepanski, M., Lee, Y.J., 2008. Role of Bax in quercetin-induced apoptosis in human prostate cancer cells. Biochem. Pharmacol. 75, 2345–2355.
Letchoumy, P.V., Mohan, K.V., Prathiba, D., Hara, Y., Nagini, S., 2007. Comparative evaluation of antiproliferative, antiangiogenic and apoptosis inducing potential of black tea polyphenols in the hamster buccal pouch carcinogenesis model. J. Carcinog. 6, 19.
Logue, S.E., Martin, S.J., 2008. Caspase activation cascades in apoptosis. Biochem. Soc. Trans. 36, 1–9.
Mihara, M., Erster, S., Zaika, A., Petrenko, O., Chittenden, T., Pancoska, P., Moll, U.M., 2003. p53 has a direct apoptogenic role at the mitochondria. Mol. Cell 1, 552–554.
Mita, A.C., Mita, M.M., Nawrocki, S.T., Giles, F.J., 2008. Survivin: key regulator of mitosis and apoptosis and novel target for cancer therapeutics. Clin. Cancer Res. 14, 5000–5005.
Mosmann, T., 1983. Rapid colorimetric assay for cellular growth and survival: application to proliferation and cytotoxicity assays. J. Immunol. Methods 65, 55–63.
Murakami, A., Ashida, H., Terao, J., 2008. Multitargeted cancer prevention by quercetin. Cancer Lett. 269, 315–325.
Naugler, W.E., Karin, M., 2008. NF-kappaB and cancer-identifying targets and mechanisms. Curr. Opin. Genet. Dev. 18, 19–26.
Pahl, H.L., 1999. Activators and target genes of Rel/NF-kappaB transcription factors. Oncogene 18, 6853–6866.
Plati, J., Bucur, O., Khosravi-Far, R., 2008. Dysregulation of apoptotic signaling in cancer: molecular mechanisms and therapeutic opportunities. J. Cell. Biochem. 104, 1124–1149.
Ranelletti, F.O., Ricci, R., Larocca, L.M., Maggiano, N., Capelli, A., Scambia, G., Benedetti-Panici, P., Mancuso, S., Rumi, C., Piantelli, M., 1992. Growth-inhibitory effect of quercetin and presence of type-II estrogen-binding sites in human colon-cancer cell lines and primary colorectal tumors. Int. J. Cancer 50, 486–492.
Schultz, D.R., Harrington Jr., W.J., 2003. Apoptosis: programmed cell death at a molecular level. Semin. Arthritis Rheum. 32, 345–369.
Sethi, G., Sung, B., Aggarwal, B.B., 2008. Nuclear factor-kappaB activation: from bench to bedside. Exp. Biol. Med. 233, 21–31.
Shan, B.E., Wang, M.X., Li, R.Q., 2009. Quercetin inhibit human SW480 colon cancer growth in association with inhibition of cyclin D1 and survivin expression through Wnt/beta-catenin signaling pathway. Cancer Invest. 27, 604–612.
Shen, H.M., Tergaonkar, V., 2009. NFkappaB signaling in carcinogenesis and as a potential molecular target for cancer therapy. Apoptosis 14, 348–363.
Smiley, S.T., Reers, M., Mottola-Hartshorn, C., Lin, M., Chen, A., Smith, T.W., Steele Jr., G. D., Chen, L.B., 1991. Intracellular heterogeneity in mitochondrial membrane potentials revealed by a J-aggregate-forming lipophilic cation JC-1. Proc. Natl Acad. Sci. 88, 3671–3675.
Tanigawa, S., Fujii, M., Hou, D.X., 2008. Stabilization of p53 is involved in quercetin-induced cell cycle arrest and apoptosis in HepG2 cells. Biosci. Biotechnol. Biochem. 72, 797–804.
Wang, I.K., Lin-Shiau, S.Y., Lin, J.K., 1999. Induction of apoptosis by apigenin and related flavonoids through cytochrome c release and activation of caspase-9 and caspase-3 in leukaemia HL-60 cells. Eur. J. Cancer 35, 1517–1525.
Watson, J.L., Greenshields, A., Hill, R., Hilchie, A., Lee, P.W., Giacomantonio, C.A., Hoskin, D.W., 2010. Curcumin-induced apoptosis in ovarian carcinoma cells is p53-independent and involves p38 mitogen-activated protein kinase activation and downregulation of Bcl-2 and survivin expression and Akt signaling. Mol. Carcinog. 49, 13–24.
Yang, J.H., Hsia, T.C., Kuo, H.M., Chao, P.D., Chou, C.C., Wei, Y.H., Chung, J.G., 2006. Inhibition of lung cancer cell growth by quercetin glucuronides via G2/M arrest and induction of apoptosis. Drug Metab. Dispos. 34, 296–304.
Yip, K.W., Reed, J.C., 2008. Bcl-2 family proteins and cancer. Oncogene 27, 6398–6406.
Yoshida, M., Yamamoto, M., Nikaido, T., 1992. Quercetin arrests human leukemic T-cells in late G1 phase of the cell cycle. Cancer Res. 52, 6676–6681.
Zhang, Q., Zhao, X.H., Wang, Z.J., 2009. Cytotoxicity of flavones and flavonols to a human esophageal squamous cell carcinoma cell line (KYSE-510) by induction of G2/M arrest and apoptosis. Toxicol. In Vitro 23, 797–807.
Zhang, W., Zhang, F., 2009. Effects of quercetin on proliferation, apoptosis, adhesion and migration, and invasion of HeLa cells. Eur. J. Gynaecol. Oncol. 30, 60–64.